THE JOURNAL OF PHYSICAL CHEMISTRY B

Article

pubs.acs.org/JPCB

Dimerization of Nucleic Acid Hairpins in the Conditions Caused by Neutral Cosolutes

Shu-ichi Nakano,*[,†,‡] Hidenobu Hirayama,[†] Daisuke Miyoshi,[†,‡] and Naoki Sugimoto*[,†,‡]

[†]Faculty of Frontiers of Innovative Research in Science and Technology (FIRST) and [‡]Frontier Institute for Biomolecular Engineering Research (FIBER), Konan University, 7-1-20, Minatojima-minamimachi, Chuo-ku, Kobe 650-0047, Japan

Supporting Information

ABSTRACT: Characterization of metal ion binding to RNA and DNA base pairs is important for understanding their energy contribution to the folding and conformational changes of nucleic acid structures. In this study, we examine the equilibrium shift from the hairpin toward the dimer formation, induced by nonspecifically bound metal ions. The hairpin dimerization is markedly enhanced in the presence of high background concentrations of poly(ethylene glycol) (PEG) and several small organic molecules. The simple volume exclusion effect and the base pair stability cannot entirely account for this increase. We find that the dielectric constant correlates well with the dimerization efficiency in the conditions caused by small alcohol molecules and amide compounds as well as PEG. The hairpin dimerization experiments reveal the potential of PEG for enhancing the binding affinity between nucleic acids and metal ions, by reducing the solution dielectric constant without decreasing the thermodynamic stability of nucleic acid structures. The results presented here contribute to the understanding of nucleic acid folding and its ability to switch between alternative conformations under the condition of limited cation availability and cellular physiology.

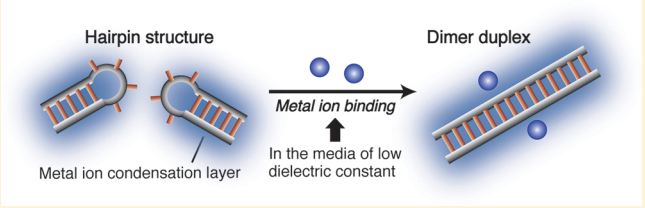

INTRODUCTION

The biological functions of RNA molecules are determined by their folding structures and often regulated by conformational changes as seen in ribozymes, riboswitches, and retrovirus RNAs.[1−3] Changes in the DNA folding conformation, such as partial refolding of genomic DNA into noncanonical structures (e.g., hairpin structure, left-handed Z-form, triplex, and quadruplex), are relevant to gene regulation, genomic instability, and genetic diseases.[4] Many structural transitions are induced by specific and nonspecific cation binding, reducing the electrostatic repulsion of phosphate charges, which allows for the creation of a more compact structure. For the formation of Watson−Crick base pairs, metal ions associate through electrostatic interactions in the counterion layer near the nucleic acid surface. Characterization of the metal ion binding during base pair formation is important for the understanding of folding pathways and thermodynamics of nucleic acid interactions.[5−7]

Dimerization of two RNA hairpins by intermolecular base pairing occurs in retroviral genomes.[1] The dimerization region contains a self-complementary sequence that either adopts a hairpin structure or forms a homodimer duplex. For instance, the dimer initiation structure (DIS) of type 1 human immunodeficiency virus (HIV-1) consists of a hairpin structure formed by a partly self-complementary 9-nt loop sequence near the 5′ end of the genomic RNA. One of the essential events in the life cycle of retroviruses is the interaction between the DIS sites initiating the dimerization of two genomic RNA molecules.[8−10] This process is enhanced in the presence of a basic nucleocapsid protein NCp7 or a large amount of metal ions.[11−14] The hairpin dimerization is also assumed to be involved in the folding pathway of guanine quadruplex DNAs.[15] Although the role of metal ions in the folding and the structure, kinetics, and thermodynamics of RNA and DNA hairpins have been extensively studied (reviewed in refs 16 and 17), the details of their contribution to the hairpin dimerization remain elusive.

In our previous study, we have reported that the hairpin structure of self-complementary DNA oligonucleotides dimerizes efficiently at high salt concentrations and in the presence of multivalent cations.[18,19] This observation can be explained by the binding of cations causing a shift in the equilibrium toward the dimer duplex formation. Such a change can be achieved by reducing the negative charge of the loop phosphodiester backbone forming Watson−Crick base pairs in the resultant dimer. In this study, we explore the self-complementary RNA and DNA oligonucleotides useful for understanding the process of the hairpin dimerization. We also examine the effect of cosolutes on the dimerization of hairpin structures. Solutions containing large amounts of cosolutes have been used to mimic the intracellular environment, normally crowded by macromolecules, and to alter the properties of solutions.[20,21] Oligonucleotide reactions such as hybridization and folding and their thermodynamics are influenced by neutral coso-

Received: March 6, 2012
Revised: June 3, 2012
Published: June 15, 2012

lutes.[22−26] Here, we demonstrate increased efficiency of the dimerization of RNA and DNA hairpins in concentrated solutions of neutral cosolutes, particularly high molecular weight poly(ethylene glycol) (PEG). We suggest that the cosolute effect is primarily attributed to the decreased dielectric permittivity, rather than the excluded volume effect and the changes in water activity and viscosity. The results show the potential of PEG for enhancing the binding affinity between nucleic acids and metal ions. Our data also provide important insights into the ability to switch between alternative conformations of nucleic acids in the conditions resembling a living cell environment.

MATERIALS AND METHODS

Sample and Buffer Preparation. Oligomer RNAs labeled with 6-carboxylfluorescein (6-FAM) at the 5′ end were synthesized chemically and purified by polyacrylamide gel electrophoresis (PAGE). Oligomer DNAs of high-performance liquid chromatography (HPLC) grade purity, labeled with 6-FAM at the 5′ end, were purchased from Hokkaido System Science. All reagents used for preparing the buffer solutions were purchased from Wako Pure Chemical Industries, except for Na_2EDTA (disodium salt of ethylenediamine-*N*,*N*,*N*′,*N*′-tetraacetic acid) which was purchased from Dojindo, PEG8000 (PEG with an average molecular weight of 8×10^3) from MP Biomedicals, dextran from Sigma, and 2-methoxyethanol from TCI. These reagents were used without further purification.

The buffer solution contained 25 mM HEPES (4-(2-hydroxyethyl)-1-piperazineethanesulfonic acid), 0.1 mM Na_2EDTA, and appropriate amounts of metal ions and cosolute molecules, unless stated otherwise. For the experiments using $MgCl_2$, $[Co(NH_3)_6]Cl_3$, or polyamine, 10 mM NaCl was included in the solution. The pH of the reaction buffer was adjusted to 7.0 at 37 °C after the addition of a cosolute molecule.

Analysis of the Secondary Structure of Oligonucleotides Using the Polyacrylamide Gel Electrophoresis. Oligonucleotides at 1 or 0.1 μM concentration, unless mentioned specifically, were annealed by lowering the temperature from 90 to 37 °C at the rate of −1 °C min^{-1} to establish the conformational equilibrium, where the annealing rate did not affect the equilibrium of the structures. According to the melting and annealing curves obtained by monitoring the UV absorption, the denaturation and renaturation were reversible. For the $MgCl_2$ experiments, we used the buffer solution without Na_2EDTA and the annealing was performed starting from 75 °C to avoid the hydrolysis of RNA. After annealing, the sample was loaded onto a native 20% polyacrylamide gel (acrylamide:bisacrylamide = 19:1) at 37 °C. We used the TBE running buffer at pH 8.3 containing 0.09 M tris (tris-(hydroxymethyl)aminomethane), 0.09 M boric acid, and 2 mM Na_2EDTA. The fluorescence of gel stains was visualized and quantified with a fluorescent image analyzer (Fujifilm, FLA-7000).

The half-maximum concentration of metal ions required for the dimer duplex formation ($[M]_{0.5}$) was calculated by fitting to the equation $f_D = \{4[M]_0^n + K_T/C_t - (8[M]_0^n K_T/C_t + K_T^2/C_t^2)^{0.5}\}/4[M]_0^n$, where f_D is the fraction of strands in the dimer duplex and n is the binding cooperativity parameter. K_T is the thermodynamic equilibrium constant ($K_T = [H]^2[M]^n/[D] = C_t[M]^n_{0.5}$, where $[M]_{0.5}$ is the half-maximum concentration of the metal ion required for the dimer formation) for the reaction $2H + nM \rightleftharpoons D$ (H, M, and D indicate the hairpin, metal ion, and the dimer duplex, respectively). The metal ion concentration ($[M]_0$) was set to exceed the oligonucleotide strand concentration (C_t).

The energy parameter for the structural transition was calculated using the $[M]_{0.5}$ values according to the equation $\Delta G^\circ_M = -nRT\ln[M]_{0.5}$.[27] However, the n value is strongly affected by deviated experimental data because the value is calculated from the shape of a sigmoid curve. Since the experimentally obtained values of n were close to 1, we used the equation by taking $n = 1.0$. This analysis provides the data for a single ion binding and allows the comparison of the free energy values for different metal ions.

Measurements of the Solution Properties. The solution properties were examined using the HEPES buffer containing 1 M NaCl and 20 wt % cosolute at 25 °C. The solution viscosity was measured with a viscometer (A&D, SV-10). The water activity was determined by the osmotic stress method using vapor phase osmometry (Wescor pressure osmometer, 5520XR) or freezing point depression osmometry (Halbmikro osmometer, Typ Dig·L). The dielectric constant was calculated according to an equation reported by Oster utilizing the dielectric constant of a pure solvent and the mean molar polarization of a mixture solution.[28] For cosolutes where the dielectric constant of a pure solvent was unavailable in literature, the value was determined experimentally. Since a liquid dielectric constant meter cannot be used for solutions containing high salt or PEG, a fluorescent probe 1,8-ANS (1-anilino-8-naphthalene sulfonate) was employed in such solutions. The probe molecule responds to changes in dielectric property of a solution by a blue shift in the emission maximum, particularly in the media of low dielectric constant.[29] The fluorescence emission spectra with excitation at 356 nm were measured using a fluorometer (JASCO, F-6500). The dielectric constant was calculated using the standard curve for several organic solvents with known values.[30] The dielectric constant determined from the fluorescence measurement agreed (with a maximum difference of 5) with those calculated using Oster's equation, except for amide compounds, possibly due to a direct interaction with 1,8-ANS.

Measurement and Analysis of the Thermal Melting Data. The thermal melting curve of an RNA duplex at 2 μM concentration was obtained in the 10 mM Na_2HPO_4 buffer at pH 7.0, containing 1 M NaCl and 1 mM Na_2EDTA, using a spectrophotometer equipped with a temperature controller (Shimadzu, UV1800). Before the measurement, oligonucleotides were heated to 90 °C and cooled to 0 °C at the rate of −2 °C min^{-1}. The UV melting curve was monitored at 260 nm at a heating rate of 0.5 °C min^{-1}. The melting temperature (T_m) at which half of the duplex structure is dissociated was determined by fitting the melting curve to the theoretical curve programmed for an intermolecular transition.[31]

RESULTS

Hairpin Dimerization of the RNA Sequence Derived from the HIV-1 DIS. Self-complementary oligonucleotides can adopt a hairpin structure and form a homodimeric duplex in equilibrium, depending on the sequence and salt concentration.[18] We investigated the secondary structure of a self-complementary 23-mer RNA fragment derived from the DIS of HIV-1. The RNA structure was equilibrated by thermal annealing in solutions of different compositions. The RNA sequence remains in a conformational equilibrium between the unimolecular hairpin loop and the bimolecular structure with

dx.doi.org/10.1021/jp302170f | J. Phys. Chem. B 2012, 116, 7406−7415

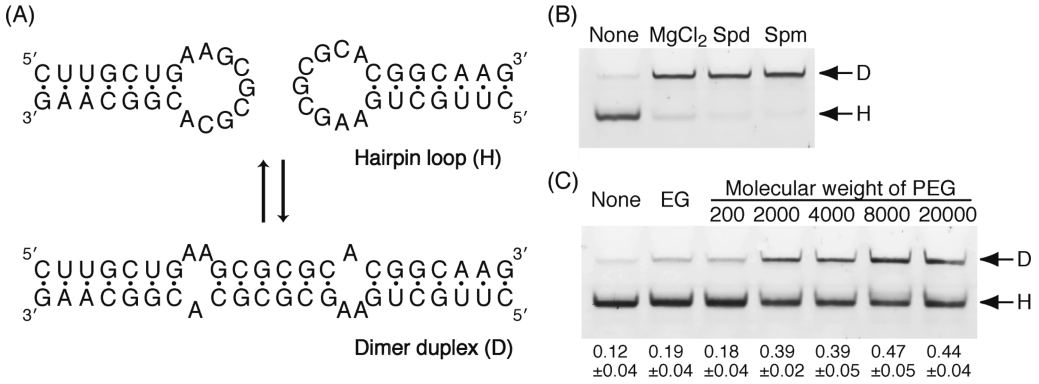

Figure 1. (A) Secondary structures of the HIV-1 DIS RNA fragment used in this study. (B) PAGE image for the fluorescently labeled RNA at 50 nM concentration in 10 mM NaCl with and without $MgCl_2$, spermidine (Spd), or spermine (Spm) at 1 mM. The fluorescent bands H and D represent the hairpin and the dimer duplex, respectively. (C) PAGE image obtained in 10 mM NaCl, in the absence and presence of 20 wt % EG or PEG with molecular weights in the range of 200−20000. The fractions of the dimer duplex determined from triplicate measurements are given underneath the picture.

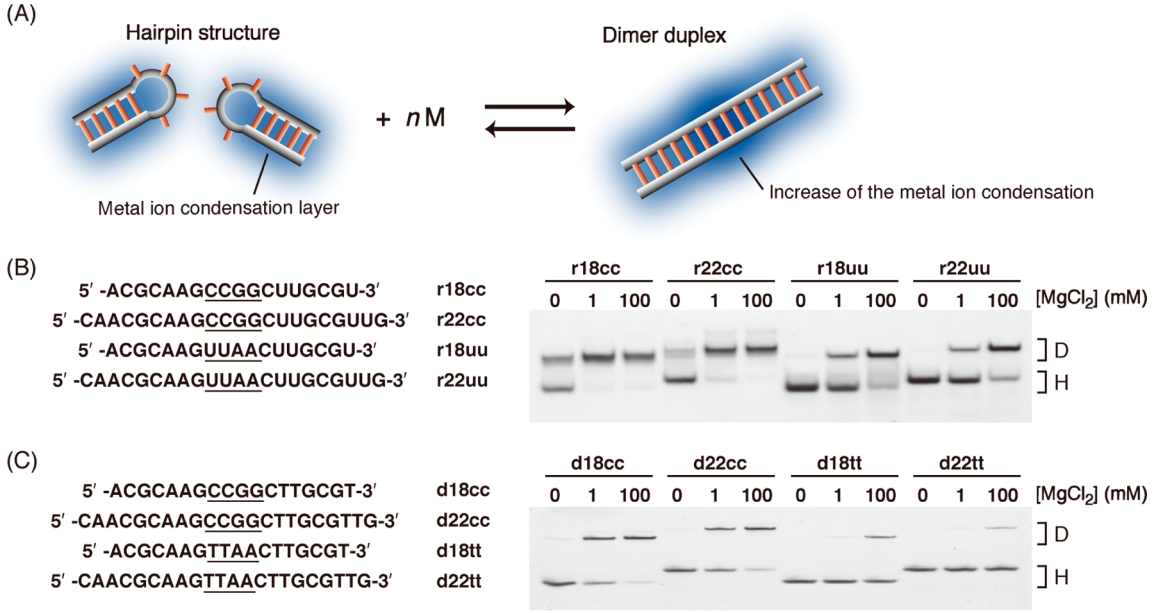

Figure 2. (A) Reaction equilibrium for the hairpin dimerization accompanied by the binding of metal ion M. The number of cooperatively bound metal ions is represented by *n*. (B) Self-complementary RNA sequences and their mobility in the polyacrylamide gel. The putative hairpin loop nucleotides are underlined. The RNA samples were prepared in 10 mM NaCl and 0, 1, or 100 mM $MgCl_2$. The hairpin and the dimer duplex are labeled as H and D, respectively. (C) Self-complementary DNA sequences and their mobility in the polyacrylamide gel.

two internal loops, as shown in Figure 1A. The mobility of the hairpin structure and the dimer duplex is different in polyacrylamide gel. We find that the hairpin structure is predominantly formed in 10 mM NaCl whereas complete dimerization takes place in solutions containing the multivalent cation of Mg^{2+}, spermidine, or spermine (Figure 1B). Remarkably, the dimerization also takes place in the presence of high concentrations of background neutral molecules. We employed different sizes of PEG (ranging in molecular weight from 200 to 2×10^4) and ethylene glycol (EG) as a monomer unit of PEG. The fraction of the dimer duplex increased gradually with the increasing PEG size (Figure 1C) and amount (Figure S1).

Fully Self-Complementary Oligonucleotides Showing the Structural Transition. The hairpin dimerization at a high metal ion concentration or in the presence of multivalent cations can be accounted for by the screening of electrostatic repulsion of the loop nucleotides once in a duplex structure. Cation association enables base pairing between the loop nucleotides to form the dimer duplex, where counterion condensation is more significant on the Watson−Crick base pairs than on the unpaired loop nucleotides (Figure 2A). Thus, the shift in the hairpin−duplex equilibrium caused by changing the metal ion concentration can be used for the evaluation of the interaction between a nucleotide and the ion. However, when either the hairpin or the dimer is extremely stable, the transition between the two structures becomes incomplete because of the requirement of very high or low salt concentration out of the range studied in this work. Such an oligonucleotide is unsuitable for quantitative analysis, which is the case for the RNA sequence derived from the HIV-1 DIS.

To explore oligonucleotide sequences that exhibit a complete transition within the experimental metal ion concentration range, we examined fully self-complementary RNA sequences.

dx.doi.org/10.1021/jp302170f | J. Phys. Chem. B 2012, 116, 7406−7415

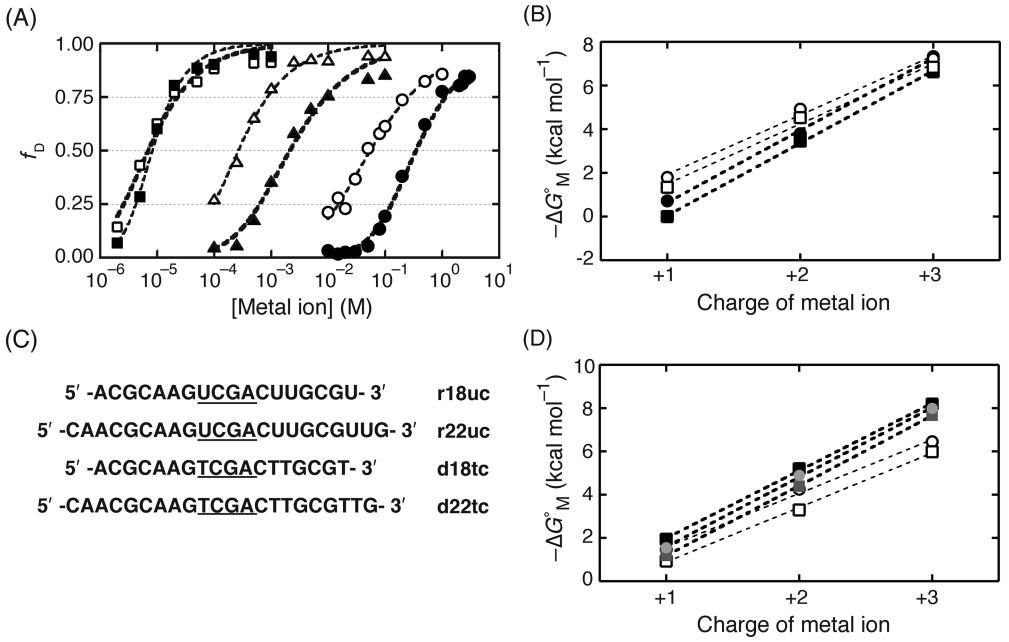

Figure 3. (A) Fraction of the dimer duplex f_D for r18uu (filled symbols) and d18cc (empty symbols) at 1 μM concentration, for different concentrations of NaCl (circles), $MgCl_2$ (triangles), and $[Co(NH_3)_6]Cl_3$ (squares). The broken lines indicate the curve fitting assuming the two-state transition for r18uu (thick) and d18cc (thin). (B) Plots of the dimerization energy $-\Delta G^{\circ}_M$ against the ionic charge of sodium, magnesium, and cobalt hexamine for r18uu (filled circles), r22uu (filled squares), d18cc (empty circles), and d22cc (empty squares) at 1 μM. The error in each data point is smaller than the size of the symbols in the plots. The linear regression analysis provides the slopes of 3.3 ± 0.1, 3.3 ± 0.1, 2.7 ± 0.3, and 2.7 ± 0.2, respectively. (C) Self-complementary sequences of RNA and DNA oligonucleotides containing the central tetranucleotides of UCGA or TCGA. (D) Plots of the dimerization energy $-\Delta G^{\circ}_M$ against the charge of metal ion for r22uc (filled squares), d18tc (empty circles), and d22tc (empty squares) at 1 μM. The squares and circles filled with gray represent the data for r22uc and r18uc, respectively, at 0.1 μM concentration. The linear regression analysis provides the slopes of 3.1 ± 0.1, 2.5 ± 0.2, 2.5 ± 0.1, 3.2 ± 0.1, and 3.2 ± 0.1, respectively.

Such sequences form a dimer duplex without unpaired nucleotides where metal ions may bind specifically. We used the oligonucleotides with a length of 18- or 22-mer to stabilize their secondary structures even at low metal ion concentrations. Each oligonucleotide has a tetranucleotide sequence in the center, either CCGG (r18cc and r22cc) or UUAA (r18uu and r22uu), as presented in Figure 2B. Importantly, the putative loop of the hairpin structures contain CCGG or UUAA, and the tetranucleotide sequence affects the stability of the dimer duplex much more than the stability of the hairpin structure. These oligonucleotides change the secondary structure depending on the metal ion concentration: r18uu and r22uu form mainly the hairpin structure in 10 mM NaCl and the dimer duplex in 100 mM $MgCl_2$, while r18cc and r22cc partly dimerize even in 10 mM NaCl (Figure 2B). Notably, the secondary structures that had annealed in 10 mM NaCl or 1 mM $MgCl_2$ were retained despite the subsequent addition of $MgCl_2$ or EDTA, respectively (Figure S2). This result indicates that the rates of interconversion and dissociation of the folded structures are extremely low and the secondary structures remain unchanged during electrophoresis.

Figure 2C shows the PAGE pattern for the corresponding DNA sequences containing the central tetranucleotides CCGG or TTAA. Unlike the RNA oligonucleotides, d18tt and d22tt containing TTAA mostly form the hairpin structure even with 100 mM $MgCl_2$, but d18cc and d22cc containing CCGG show an almost complete transition from the hairpin to the dimer duplex with the increasing $MgCl_2$ concentration.

Energy of the Structural Transition from the Hairpin to the Dimer Duplex. We studied the structural transition in more detail using r18uu and d18cc, that changed the secondary structure by increasing the concentration of Na^+ and $[Co(NH_3)_6]^{3+}$ as well as Mg^{2+}. The dimer fraction of r18uu and d18cc increased with the increasing amount and ionic charge of metal ions, and the hairpin to dimer transition agreed well with the curve fitting assuming the two-state process, as shown in Figure 3A. The plot gives the half-maximum concentration of metal ions required for the dimer formation ($[M]_{0.5}$) and the number of cooperatively bound ions (n). The value of $[M]_{0.5}$ becomes lower with the increasing metal ion charge. The RNA sequence r18uu has larger values of $[M]_{0.5}$ for Na^+ and Mg^{2+} than the DNA sequence d18cc, but their values for $[Co(NH_3)_6]^{3+}$ are similar. The n values for all the ions were within the range of 1.2−1.7, indicating an almost noncooperative interaction. The apparent energies required for the structural transitions of r18uu, d18cc, r22uu, and d22cc were calculated using the $[M]_{0.5}$ values. We obtained the linear plots of the energy parameter ΔG°_M against the metal ion charge, demonstrating the slope of 3.3 kcal mol^{-1} (1 kcal = 4.18 kJ) for r18uu and r22uu, and the slope of 2.7 kcal mol^{-1} for d18cc and d22cc (Figure 3B).

To compare the transition energy for RNA and DNA of the same sequence, different oligonucleotide sequences were tested. Finally, we found the 18-mer and 22-mer sequences containing the central tetranucleotides UCGA for RNA (r18uc and r22uc) and TCGA for DNA (d18tc and d22tc), presented in Figure 3C. These sequences formed the hairpin structure in 10 mM NaCl and the dimer duplex in 1 M NaCl or 100 mM $MgCl_2$ (Figure S3A), allowing the curve-fitting analysis for the binding of Na^+ and Mg^{2+}. However, r18uc and r22uc showed a mixture of the hairpin and the dimer duplex at the low concentrations of $[Co(NH_3)_6]^{3+}$. For the curve-fitting analysis, the metal ion

dx.doi.org/10.1021/jp302170f | J. Phys. Chem. B 2012, 116, 7406−7415

concentration has to be higher than the concentration of oligonucleotides. We used 1 μM oligonucleotide concentration in most cases but also performed some experiments with the 0.1 μM RNA concentration. In the experiments with the lowered RNA concentration, we observed the increase in the metal ion concentration required for the hairpin dimerization and the hairpin structure was predominant at the submicromolar concentration of $[Co(NH_3)_6]^{3+}$, allowing for the accurate curve-fitting analysis (Figure S3B). Table 1 shows the $[M]_{0.5}$ values for r22uc, including the values for other ions (Li^+, K^+, Rb^+, Cs^+, NH_3^+, Ca^{2+}, Sr^{2+}, and Ba^{2+}). Strikingly, the concentration required for the hairpin dimerization was similar for metal ions with the same charge, and the n values were within the range of 1.1−1.7. The results suggest that the metal ion binding required for the hairpin dimerization is predominantly caused by nonspecific electrostatic interactions with a weak binding cooperativity.

Table 1. Half-Maximum Concentration of Metal Ions Required for the Hairpin Dimerization of r22uc[a]

metal ion	$[M]_{0.5}$ (mM)	metal ion	$[M]_{0.5}$ (mM)
Li^+	110 ± 7	Mg^{2+}	0.80 ± 0.10
Na^+	140 ± 10	Ca^{2+}	0.69 ± 0.09
K^+	170 ± 10	Sr^{2+}	0.98 ± 0.10
Rb^+	170 ± 12	Ba^{2+}	0.96 ± 0.10
Cs^+	170 ± 11	$[Co(NH_3)_6]^{3+}$	0.0057 ± 0.0006
NH_3^+	150 ± 8		

[a]The experiments were performed with the RNA concentration at 0.1 μM. The n values for all ions were within the range of 1.1−1.7.

The linear plots in Figure 3D give the free energy changes of the new oligonucleotides for increasing metal ion charges, 3.2 kcal mol^{-1} for the RNAs regardless of their concentration (Figure 3D) and 2.5 kcal mol^{-1} for the DNAs. Strikingly, the changes for the RNA oligonucleotides r18uc and r22uc are similar to those for r18uu and r22uu, as are those within the DNA oligonucleotides of d18tc, d22tc, d18cc, and d22cc. It can be concluded that the free energy change for RNA sequences is 0.6−0.7 kcal mol^{-1} greater than that for DNA sequences, independent from the oligonucleotide length and the loop sequence.

Effect of PEG on the Hairpin Dimerization. The metal ion concentrations required for the hairpin dimerization were further obtained using concentrated solutions of cosolutes. Neutral cosolutes have been used in mimicking intracellular conditions, such as macromolecular crowding, viscous fluid media, and altered molecular activities.[20,32,33] In particular, PEG is useful because of its high solubility in water and availability of the products with different molecular weights. It is regarded that the interaction of metal ions with PEG becomes significant only in solutions containing a considerable amount of organic solvent,[34] but this is not the case in this study.

The RNA sequence r22uc forms the hairpin structure in 10 mM NaCl, but the fraction of the dimer duplex increases when PEG is added to the low salt solution (Figure 4A), as observed with the HIV-1 DIS fragment sequence. Dimerization increases with increasing molecular weight and amount of PEG, leading to a predominant dimer formation of PEG with an average molecular weight of 8000 (PEG8000) at a concentration of 40 wt %. We can conclude that the large PEG effectively induces the dimerization even with limited availability of metal ions. Figure 4B shows a 5-fold decrease in the half-maximum concentration of Na^+ and a 17-fold decrease in the case of Mg^{2+} for the dimerization of r22uc with 20 wt % PEG8000. The profiles for the structural transitions of r22uc and d22tc by

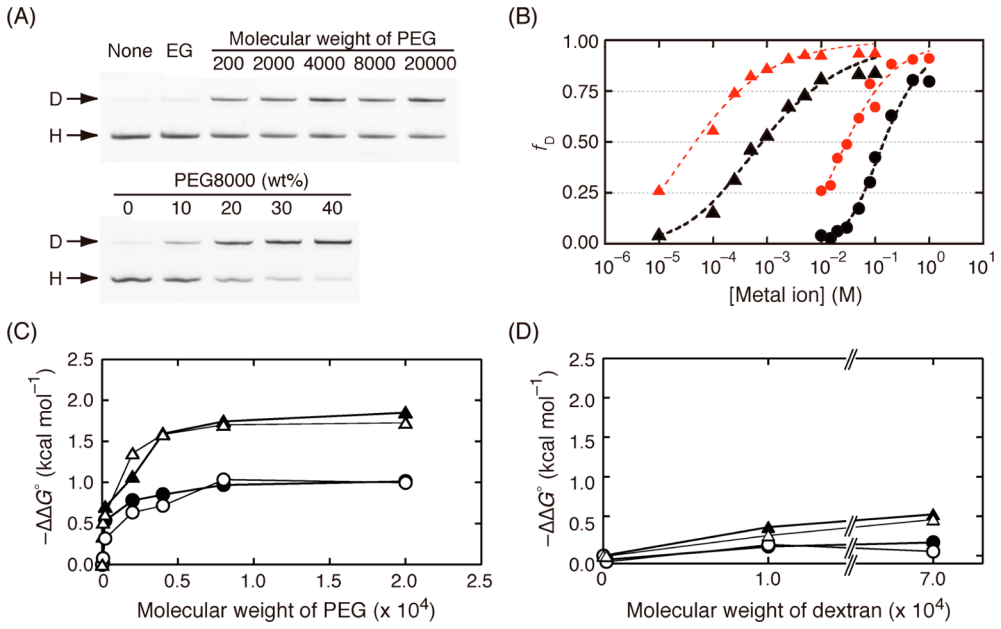

Figure 4. (A) PAGE images for r22uc in 10 mM NaCl, in the absence and presence of EG or PEG at 20 wt % (upper image) or different amounts of PEG8000 (lower image). (B) Fraction of the dimer duplex of r22uc for different concentrations of NaCl (circles) and $MgCl_2$ (triangles) in the absence (black) and presence of 20 wt % PEG8000 (red). (C) Changes in ΔG°_M for the dimerization of r22uc (filled symbols) and d22tc (empty symbols) by Na^+ (circles) or Mg^{2+} (triangles) in the presence of 20 wt % EG or PEGs of different molecular weights, represented by $\Delta\Delta G^\circ$ [= ΔG°_M(with cosolute) − ΔG°_M(without cosolute)]. The data for EG is plotted at the molecular weight of 62. (D) Free energy for the dimerization of r22uc (filled symbols) and d22tc (empty symbols) in the presence of Na^+ (circles) or Mg^{2+} (triangles) in the solutions containing 20 wt % glucose or dextran of different molecular weights. The data for glucose is plotted at the molecular weight of 180.

dx.doi.org/10.1021/jp302170f | J. Phys. Chem. B 2012, 116, 7406−7415

other divalent ions also provide reduced $[M]_{0.5}$ values (9−17-fold) in the presence of PEG, as shown in Table 2.

Table 2. Half-Maximum Concentration $[M]_{0.5}$ (mM) of Divalent Metal Ions for the Dimer Formations of r22uc and d22tc without and with 20 wt % PEG8000[a]

metal ion	without	with PEG
	For r22uc	
Mg^{2+}	0.80 ± 0.10	0.047 ± 0.006
Ca^{2+}	0.69 ± 0.09	0.052 ± 0.017
Sr^{2+}	0.98 ± 0.10	0.060 ± 0.015
Ba^{2+}	0.96 ± 0.10	0.068 ± 0.014
	For d22tc	
Mg^{2+}	4.7 ± 1.0	0.30 ± 0.02
Ca^{2+}	4.1 ± 0.6	0.43 ± 0.05
Sr^{2+}	3.8 ± 0.3	0.29 ± 0.06
Ba^{2+}	4.3 ± 0.8	0.47 ± 0.07

[a]The experiments were performed with 0.1 μM for r22uc and 1 μM for d22tc. The *n* values were within the range of 0.7−1.3.

The changes in ΔG°_M for the hairpin dimerization of r22uc and d22tc after adding 20 wt % PEG or EG, $-\Delta\Delta G^\circ$, are compared in Figure 4C. The value increases with increasing PEG size but reaches saturation at about 1.0 kcal mol^{-1} for Na^+ and 1.7 kcal mol^{-1} for Mg^{2+} with PEG larger than 2000−4000. The similar energy profiles were also obtained with the 18-mer oligonucleotides, r18uu and d18cc (data not shown). Table 3

Table 3. Increments in the Free Energy Change for the Hairpin Dimerization $-\Delta\Delta G^\circ$ (kcal mol^{-1}) of the Self-Complementary Oligonucleotides after Adding 20 wt % PEG8000[a]

metal ion	r18uu	r22uu	r18uc	r22uc	d18cc	d22cc	d18tc	d22tc
Na^+	1.0	1.1	0.85	0.97	1.0	1.1	1.0	1.0
Mg^{2+}	1.8	1.5	1.7	1.7	1.7	1.8	1.6	1.7

[a]Each error is within 20% of the value.

lists the $-\Delta\Delta G^\circ$ values for other sequences using 20 wt % PEG8000; they are in the range of 0.85−1.1 kcal mol^{-1} for the Na^+-induced dimerization and 1.5−1.8 kcal mol^{-1} for the Mg^{2+}-induced dimerization. In contrast, glucose and the polysaccharide dextrans with the average molecular weights of 1×10^4 (Dex10) and 7×10^4 (Dex70) showed only a small effect on $-\Delta\Delta G^\circ$, at most 0.2 kcal mol^{-1} for Na^+ and 0.5 kcal mol^{-1} for Mg^{2+} (Figure 4D). The data suggests that the enhancement of the hairpin dimerization is characteristic for high molecular weight PEGs.

Origin of the Cosolute Effect. The melting temperature T_m of the 9-mer RNA duplex 5′-CAACGCAAG-3′/5′-CUUGCGUUG-3′ derived from the stem sequence of the 22-mer hairpin RNA was measured in the PEG-containing solutions. The small-sized PEG and EG significantly decreased the base pair stability as compared with large PEGs (Figure 5A). The T_m data reflecting the thermal stability of Watson−Crick base pairs seemed unrelated to the PEG effect on the hairpin dimerization. This conclusion is supported by the T_m data obtained with other cosolute molecules described later.

We compared the property parameters of solutions containing EG and PEG (Figure S4). Viscosity and water activity were measured using a viscometer and osmometer, respectively. The viscosity increases progressively with the increasing molecular weight of PEG. The water activity for EG and small PEGs decreases more than those for large PEGs. The solution viscosity affects the probability of molecular collision and bimolecular association rates, and the change of water activity alters the equilibrium of reactions that accompany water uptake or release. However, these properties do not account for the observed PEG effect, which is the increased dimer formation with larger PEGs and saturation at the molecular weights of 2000 and above.

After the addition of PEG, the relative dielectric constant ε_r of a solution decreases.[35] Larger PEGs change the ε_r down to 57 by PEG8000 and 54 by PEG20000 at 20 wt % (evaluation using a fluorescent probe 1,8-ANS), but the value changes are relatively small for PEG sizes of 2000 and above. This saturation behavior is consistent with the structural aspect that a larger fraction of PEG monomers is buried inside a flexible coil of the longer polymers. We find that the inverse of the relative dielectric constant ε_r^{-1} scales well with the PEG size-dependence data shown in Figure 4C. The glucose and dextran solutions show relatively smaller changes in the dielectric constant, in agreement with the data indicated in Figure 4D. To investigate the role of the dielectric constant in the hairpin dimerization, we tested several small molecules (Figure S5A). Ethylene glycol derivatives of 1,3-propanediol (PDO), 2-methoxyethanol (MME), and 1,2-dimethoxyethane (DME) destabilized the Watson−Crick base pairs of the 9-mer duplex equal to or more than EG (Figure 5A), and the molecules change the dielectric constant to 70−62. Consistent with the ε_r data, these compounds increased the dimerization efficiency of r22uc and d22tc. The same observation was made when the small alcohol molecules of methanol (MeOH), ethanol (EtOH), 1-propanol (PrOH), and 2,2,2-trifluoroethanol (TFE) were used (Figure S5B). As some amide compounds have unusual dielectric properties,[30] we also tested formamide (FA), *N*-methylformamide (NMF), and *N*,*N*-dimethylformamide (DMF). Figure 5A shows that these compounds destabilize the RNA duplex to a similar extent. The dielectric constant of the solutions containing FA and NMF is increased to 84 and 100, respectively (calculated using Oster's equation[28] because 1,8-ANS could not be used, see the Materials and Methods section). With these compounds, the metal ion concentration required for the hairpin dimerizations increased. In contrast, DMF decreases the dielectric constant to 65 and reduced the metal ion concentration required for the dimer formation (Figure S5C). We further examined dimethyl sulfoxide (DMSO) and tetrahydrofulane (THF), having no carbonyl or hydroxyl group within the molecule. These are the typical organic solvents having a relatively high or low polarity. As expected from the dielectric constant, DMSO provided relatively small effects and THF increased the dimerization efficiency. These observations fairly agree with the idea that the dielectric constant has a direct relevance to the PEG effect on the hairpin dimerization. Figure 5B shows the linear relationships between $-\Delta\Delta G^\circ$ for the Na^+- or Mg^{2+}-induced dimerizations of r22uc and d22tc and ε_r^{-1} of the cosolute-containing solutions examined in this study. The similar linear plots were also obtained for r18uu and d18cc (data not shown). Finding such linear correlations suggests that the PEG effect on the hairpin dimerization is primarily caused by enhancement of the binding affinity between nucleic acids and metal ions under the conditions of decreased dielectric permittivity.

dx.doi.org/10.1021/jp302170f | J. Phys. Chem. B 2012, 116, 7406−7415

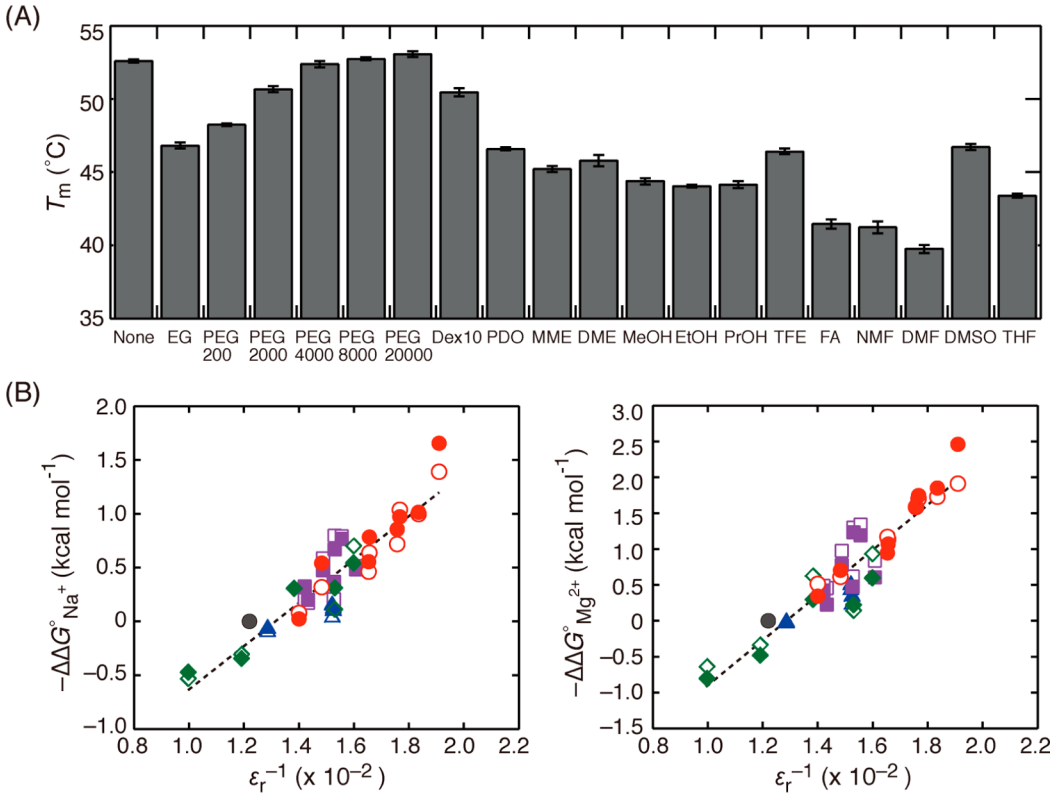

Figure 5. (A) Comparison of the melting temperature T_m of the 9-mer RNA duplex in the 1 M NaCl-phosphate buffer with and without 20 wt % cosolute. The values of T_m were obtained from the average of duplicate measurements. (B) Increments of the free energy for the hairpin dimerization of r22uc (filled symbols) and d22tc (empty symbols) for Na^+ ($-\Delta\Delta G^\circ_{Na^+}$) or Mg^{2+} ($-\Delta\Delta G^\circ_{Mg^{2+}}$) against the inverse of dielectric constant of solutions. The black symbols indicate the data for the solution without adding a cosolute. The red symbols represent the data for EG and PEG, the blue symbols represent the data for glucose and dextran, the purple symbols indicate the data for the ethylene glycol derivatives and small alcohol molecules, and the green symbols indicate the data for the amide compounds, DMSO, and THF at 20 wt %. The data obtained with 10, 30, and 40 wt % PEG8000 are also plotted. The dotted line shows the linear regression fit to the data points, giving the correlation coefficient r^2 0.83 for the Na^+ or 0.85 for the Mg^{2+} data.

DISCUSSION

Oligonucleotide Sequences for the Study of Hairpin Dimerization. A self-complementary sequence of nucleic acids has inherent conformational polymorphism, allowing the formation of an intramolecular hairpin and an intermolecular dimer duplex. The hairpin and the dimer can both be present in a state of conformational equilibrium, and the fraction of each structure depends on the oligonucleotide sequence and the solution component. We find that the formation of the dimer duplex is enhanced by employing a GC-rich loop sequence. This is because of the greater stability of the G/C base pair formed in a dimer, effectively shifting the equilibrium toward an intermolecular duplex. Notably, the loop nucleotides of dimer initiation sites of many retroviruses are GC-rich; this is also the case for the HIV-1 DIS. The results presented here suggest that the natural cellular environment, rich in proteins and other host cell components, affects the efficiency of dimerization of retrovirus genomic RNAs.

Because of stronger base pairing in RNA as compared with DNA,[36] the hairpin−duplex equilibrium of RNA is shifted more toward the dimer formation than for DNA with the same sequence. This makes it difficult to compare the dimerization energies for RNA and DNA hairpins. However, the comparison was possible for UCGA loop sequence in RNA and TCGA sequence in DNA, where the base pair interaction energy falls between those for UUAA (or TTAA) and GGCC.

Binding Property of Metal Ions Required for the Hairpin Dimerization. The hairpin dimerization is enhanced at high salt concentrations and in the presence of high valence cations. This is because the negatively charged phosphate groups of loop nucleotides must be screened for the new base pairing to occur in the dimer duplex. The formation of Watson−Crick base pairs brings the phosphates closer together, which is accompanied by an increase in the number of metal ions accumulating near the nucleic acid surface.[5,16] Thus, the metal ions inducing the structural transition from a hairpin to a dimer duplex primarily associate in the counterion layer surrounding the base pairs formed by loop nucleotides (Figure 2A). Such ions are free to move and exchange rapidly with bulk ions. The experimental system using the self-complementary sequences has important practical benefits for the study of cation binding to nucleic acids: The experiments can be systematically planned, and the relative fractions of different nucleic acid structures can be readily analyzed using PAGE. The mobility of the hairpin and the dimer duplex is distinctly different in the gel and remains unchanged during electrophoresis (Figure S2). This is consistent with the observation that the melting temperature of r22cc and r22uu (66.4 and 70.1 °C, respectively, even in 10 mM NaCl) is much higher than 37 °C used for the electrophoresis. It is also remarkable that the dynamic range of the metal ion concentration required for the structural transition can be controlled by changing the oligonucleotide concentration as well as the sequence. For

dx.doi.org/10.1021/jp302170f | J. Phys. Chem. B 2012, 116, 7406−7415

example, an incomplete transition for r22uc by $[Co(NH_3)_6]^{3+}$ can be turned into an almost complete transition within the studied ion concentration range by lowering the RNA concentration from 1 to 0.1 μM, with no change in the slope of the plot in Figure 3D.

The value of $[M]_{0.5}$ changes depending on the ionic charge, whereas the binding cooperativity is not substantially influenced. The values of ΔG°_M calculated from the $[M]_{0.5}$ show a linear relationship with the changing metal ion charge. The linearity suggests an identical mechanism for the hairpin dimerization driven by different metal ions. Since the exchange-inert metal complex $[Co(NH_3)_6]^{3+}$ has the size and coordination geometry similar to the hydrated Mg^{2+}, non-specific binding distant from the nucleotide surface plays a major role. These observations confirm that the hairpin dimerization is promoted by metal ions through electrostatic interactions in the absence of site-specific metal ion binding.

The energy parameter ΔG°_M includes contributions from the ion binding energy and the intrinsic refolding energy representing the difference in energy levels between the hairpin and the dimer duplex. From the linear plots of Figures 3B and 3D, the energy attributed to increasing the ion charge (ΔG°_{el}) can be separated from the refolding energy (ΔG°_{refold}), by assuming a simple model of the cation binding of a net charge m, represented by $\Delta G^\circ_M = \Delta G^\circ_{refold} + m\Delta G^\circ_{el}$, where ΔG°_{refold} changes with the sequence and concentration of an oligonucleotide but ΔG°_{el} does not. On the basis of the linear regression analysis, the values of ΔG°_{el} for the RNA sequences are approximately 0.6−0.7 kcal mol^{-1} greater than those for the DNA sequences, irrespective of the oligonucleotide length and sequence. This finding suggests stronger electrostatic interactions with RNA, probably caused by the presence of 2′-hydroxyl group and the helical conformation different from a typical double-helical structure of DNA. The stronger electrostatic binding with metal ions may partly account for the greater stabilization energy of RNA base pairs in comparison with DNA base pairs.[36]

Molecular Environment Created by Cosolutes. It has been demonstrated that the molecular environment created by neutral cosolutes does not change the helical conformation of a hairpin and a double-stranded duplex but affects the nucleic acid reactions, such as Watson−Crick base pairing, Hoogsteen base pairing, G-quartet structure formation, the structural transition from the B-form to the Z-form DNA, and the ribozyme catalytic activities.[22,23,26,32,37−41] This study reveals another interesting feature that the cosolutes affect the hairpin dimerization. Table 2 shows reductions of the metal ion concentration required for the hairpin dimerization in the PEG-containing solutions. The ionic radii of these metal ions vary considerably, causing substantial differences in their hydration state, hydration energy, and polarizability. Specifically, Mg^{2+} is the water structure-breaking ion and Ba^{2+} is a water structure-making ion. Nevertheless, PEG affects the $[M]_{0.5}$ of different divalent metal ions in a similar manner, suggesting that the charge density, specific metal ion coordination, and ion exclusion in the media with the reduced water activity contribute little to the PEG effect on the hairpin dimerization.

Neutral cosolutes change the free energy levels of the hairpin and the dimer duplex, as do the metal ions. The cosolute effect varies depending on chemical structure and size of the added molecules. Polymer cosolutes induce the macromolecular crowding wherein a large volume of an aqueous solution is physically occupied by cosolute molecules.[42] The dimer formation can be enhanced as a consequence of the volume exclusion by cosolutes. The theory of the excluded volume effect predicts an increase in the molecular activity with the increasing cosolute size, and the activity is progressively enhanced as the fractional volume occupancy of a cosolute increases.[42] However, the steric contribution obviously disagrees with the saturation of the PEG effect at high molecular weights and the much smaller effects of dextrans (Figures 4C and 4D). Therefore, the simple excluded volume effect cannot entirely account for the data of hairpin dimerization. On the other hand, it is proposed that PEG preferentially interacts with the nucleic acid bases exposed to a solvent.[26] The interaction is more pronounced in unpaired than in paired bases; however, this also cannot explain the enhancement of the hairpin dimerization caused by PEG. According to the thermal melting experiments, not only PEG200 and EG but also other organic molecules substantially decreased the thermal stability of the RNA duplex, while the large molecular weight PEG and dextran did not (Figure 5A). The destabilizations are accounted for by direct interactions[23,26,43,44] or by indirect repulsive interactions with an oligonucleotide.[45,46] We find that the duplex stability does not show a relationship with the dimerization efficiency, suggesting that the cosolute effect on the base pair stability is not the main determinant.

If the coordination of cosolutes to the metal ion is significant, the ion concentration required for the hairpin dimerization increases. However, most experimental results show the decrease of the concentration in the presence of cosolutes. It is thus likely that the added molecules are less likely to bind strongly to metal ions. As shown in Figure 5B, the dielectric constant correlates well with the degree of the hairpin dimerization, regardless of the added molecules. Because the plots contain the data of PEG, the interaction with PEG would contribute very little to the dimerization energy. The dielectric constant is also found to be important in DNA precipitation, DNA compaction, the torsional property of a plasmid DNA, and the binding of metal ions, e.g., Li^+, to DNA quadruplexes.[24,47−50] It is possible that the cosolute molecules modify the hydration layer of a nucleotide helix,[51] and the perturbation in the microenvironment alters the dielectric property close to nucleic acids. The used dielectric constant values would not accurately reflect the local environment near the nucleic acid surface. However, we find a good correlation with the dimerization efficiency, independent of the oligonucleotide length, nucleic acid type (RNA or DNA), and the loop sequence. The result indicates the significance of electrostatic interactions for the hairpin dimerizations in the presence of high concentrations of background molecules including PEG. The energy parameter $-\Delta\Delta G^\circ$ increases linearly with the inverse of dielectric constant ε_r^{-1}, the term proportional to the Coulomb energy: The slope of the plot is greater for Mg^{2+} than for Na^+ (Figure 5B), reflecting the stronger Coulomb interaction with Mg^{2+}.

We find that the cosolute-assisted hairpin dimerization is at least partly associated with the increased binding affinity of metal ions in the medium with lowered dielectric constant. The dielectric constant of a living cell is estimated to be around 50 or even less.[52,53] Such conditions would be favorable for the formation of base-paired structures rather than hairpin loop structures at self-complementary regions. We can speculate that the intracellular environment strongly influences the folding structure and the ability to switch between alternative

conformations of nucleic acids, which may have a significant influence not only on the dimerization efficiency of retrovirus genomic RNAs but also on the translational repression and riboswitch systems. It is also noted that large PEGs are the reagent that effectively reduces the solution dielectric constant but do not decrease the thermodynamic stability of nucleic acid structures. This is a remarkable advantage in the use of PEG as an additive for nucleic acid reactions.

CONCLUSIONS

We investigated the equilibrium shift from a hairpin to a dimer duplex of self-complementary oligonucleotides and characterized the metal ion binding to RNA and DNA in nonaqueous solutions. We show that the structural transition is affected not only by cations but also by the presence of neutral cosolutes. The structural transition is dominated by nonspecific binding of metal ions through the electrostatic interaction, and the binding energy is 0.6−0.7 kcal mol^{-1} greater for RNA compared with DNA oligonucleotides. On the other hand, the cosolute effect on the hairpin dimerization is energetically similar for RNA and DNA. We find that large PEGs effectively enhance the dimerization efficiency and the increased electrostatic interaction is primarily responsible for the PEG effect, rather than the excluded volume effect or the alterations in water activity and viscosity. The energetic aspects and the cosolute effect on the binding of nonspecifically interacting metal ions provide valuable insights into folding pathways and the thermodynamics of nucleic acid structures under the conditions where the dielectric property is lowered. Our observations reveal the importance of the solution property for RNA and DNA to switch between alternative conformations and to fulfill their physiological functions under the condition of limited cation availability and cellular physiology.

ASSOCIATED CONTENT

Supporting Information

PAGE images for the hairpin dimerizations, the property parameters of solutions containing EG and PEG, and the energy profiles for the dimerizations. This material is available free of charge via the Internet at http://pubs.acs.org.

AUTHOR INFORMATION

Corresponding Author

*E-mail shuichi@center.konan-u.ac.jp (S.N.), sugimoto@konan-u.ac.jp (N.S.); phone +81-78-303-1429; fax +81-78-303-1495.

Notes

The authors declare no competing financial interest.

ACKNOWLEDGMENTS

We thank Junpei Ueno for technical assistance. This work was supported in part by the MEXT-Supported Program for the Strategic Research Foundation at Private Universities, 2009-2014, and the Hirao Taro Foundation of the Konan University Association for Academic Research.

REFERENCES

(1) Greatorex, J. *Retrovirol* **2004**, *1*, 22.
(2) Schwalbe, H.; Buck, J.; Fürtig, B.; Noeske, J.; Wöhnert, J. *Angew. Chem., Int. Ed. Engl.* **2007**, *46*, 1212−1219.
(3) Zhang, J.; Lau, M. W.; Ferre-D'Amare, A. R. *Biochemistry* **2010**, *49*, 9123−9131.
(4) Zhao, J.; Bacolla, A.; Wang, G.; Vasquez, K. M. *Cell. Mol. Life Sci.* **2010**, *67*, 43−62.
(5) Draper, D. E. *RNA* **2004**, *10*, 335−343.
(6) Fedorova, O.; Waldsich, C.; Pyle, A. M. *J. Mol. Biol.* **2007**, *366*, 1099−1114.
(7) Woodson, S. A. *Annu. Rev. Biophys. Biomol. Struct.* **2010**, *39*, 61−77.
(8) Clever, J. L.; Wong, M. L.; Parslow, T. G. *J. Virol.* **1996**, *70*, 5902−5908.
(9) Paillart, J. C.; Westhof, E.; Ehresmann, C.; Ehresmann, B.; Marquet, R. *J. Mol. Biol.* **1997**, *270*, 36−49.
(10) Lu, K.; Heng, X.; Garyu, L.; Monti, S.; Garcia, E. L.; Kharytonchyk, S.; Dorjsuren, B.; Kulandaivel, G.; Jones, S.; Hiremath, A.; et al. *Science* **2011**, *334*, 242−245.
(11) Shubsda, M. F.; McPike, M. P.; Goodisman, J.; Dabrowiak, J. C. *Biochemistry* **1999**, *38*, 10147−10157.
(12) Takahashi, K. I.; Baba, S.; Chattopadhyay, P.; Koyanagi, Y.; Yamamoto, N.; Takaku, H.; Kawai, G. *RNA* **2000**, *6*, 96−102.
(13) Rist, M. J.; Marino, J. P. *Biochemistry* **2002**, *41*, 14762−14770.
(14) Li, P. T.; Tinoco, I., Jr. *J. Mol. Biol.* **2009**, *386*, 1343−1356.
(15) Balagurumoorthy, P.; Brahmachari, S. K.; Mohanty, D.; Bansal, M.; Sasisekharan, V. *Nucleic Acids Res.* **1992**, *20*, 4061−4067.
(16) Draper, D. E.; Grilley, D.; Soto, A. M. *Annu. Rev. Biophys. Biomol. Struct.* **2005**, *34*, 221−243.
(17) Bevilacqua, P. C.; Blose, J. M. *Annu. Rev. Phys. Chem.* **2008**, *59*, 79−103.
(18) Nakano, S.; Kirihata, T.; Fujii, S.; Sakai, H.; Kuwahara, M.; Sawai, H.; Sugimoto, N. *Nucleic Acids Res.* **2007**, *35*, 486−494.
(19) Nakano, S.; Kirihata, T.; Sugimoto, N. *Chem. Commun.* **2008**, 700−702.
(20) Luby-Phelps, K. *Int. Rev. Cytol.* **2000**, *192*, 189−221.
(21) Johansson, G.; Walter, H. *Int. Rev. Cytol.* **2000**, *192*, 33−60.
(22) Spink, C. H.; Chaires, J. B. *J. Am. Chem. Soc.* **1995**, *117*, 12887−12888.
(23) Nakano, S.; Karimata, H.; Ohmichi, T.; Kawakami, J.; Sugimoto, N. *J. Am. Chem. Soc.* **2004**, *126*, 14330−14331.
(24) Smirnov, I. V.; Shafer, R. H. *Biopolymers* **2007**, *85*, 91−101.
(25) Downey, C. D.; Crisman, R. L.; Randolph, T. W.; Pardi, A. *J. Am. Chem. Soc.* **2007**, *129*, 9290−9291.
(26) Knowles, D. B.; LaCroix, A. S.; Deines, N. F.; Shkel, I.; Record, M. T., Jr. *Proc. Natl. Acad. Sci. U.S.A.* **2011**, *108*, 12699−12704.
(27) Fang, X.; Pan, T.; Sosnick, T. R. *Biochemistry* **1999**, *38*, 16840−16846.
(28) Oster, G. *J. Am. Chem. Soc.* **1946**, *68*, 2036−2041.
(29) Barghouthi, S. A.; Perrault, J.; Holmes, L. H. *Chem. Educ.* **1998**, *3*, 1−10.
(30) Speight, J. G. *Lange's Handbook of Chemistry*, 16th ed.; McGraw-Hill: New York, 2005.
(31) Puglisi, J. D.; Tinoco, I., Jr. *Methods Enzymol.* **1989**, *180*, 304−325.
(32) Nakano, S.; Wu, L.; Oka, H.; Karimata, H. T.; Kirihata, T.; Sato, Y.; Fujii, S.; Sakai, H.; Kuwahara, M.; Sawai, H.; et al. *Mol. BioSyst.* **2008**, *4*, 579−588.
(33) Zhou, H. X.; Rivas, G.; Minton, A. P. *Annu. Rev. Biophys. Biomol. Struct.* **2008**, *37*, 375−397.
(34) Honda, H.; Ono, K.; Murakami, K. *Macromolecules* **1990**, *23*, 515−520.
(35) Arnold, K.; Herrmann, A.; Pratsch, L.; Gawrisch, K. *Biochim. Biophys. Acta* **1985**, *815*, 515−518.
(36) Bloomfield, V. A.; Crothers, D. M.; Tinoco, J. I. Interaction of Nucleic Acids and Water and Ions. In *Nucleic Acids: Structures, Properties and Functions*; University Science Books Press: Sausalito, CA, 2000; pp 475−534.
(37) Miyoshi, D.; Karimata, H.; Sugimoto, N. *Angew. Chem., Int. Ed. Engl.* **2005**, *44*, 3740−3744.
(38) Kan, Z. Y.; Lin, Y.; Wang, F.; Zhuang, X. Y.; Zhao, Y.; Pang, D. W.; Hao, Y. H.; Tan, Z. *Nucleic Acids Res.* **2007**, *35*, 3646−3653.
(39) Miyoshi, D.; Nakamura, K.; Tateishi-Karimata, H.; Ohmichi, T.; Sugimoto, N. *J. Am. Chem. Soc.* **2009**, *131*, 3522−3531.

(40) Nakano, S.; Karimata, H. T.; Kitagawa, Y.; Sugimoto, N. *J. Am. Chem. Soc.* **2009**, *131*, 16881−16888.
(41) Kilburn, D.; Roh, J. H.; Guo, L.; Briber, R. M.; Woodson, S. A. *J. Am. Chem. Soc.* **2010**, *132*, 8690−8696.
(42) Minton, A. P. *Methods Enzymol.* **1998**, *295*, 127−149.
(43) Blake, R. D.; Delcourt, S. G. *Nucleic Acids Res.* **1996**, *24*, 2095−2103.
(44) Del Vecchio, P.; Esposito, D.; Ricchi, L.; Barone, G. *Int. J. Biol. Macromol.* **1999**, *24*, 361−369.
(45) Engberts, J. B. F. N.; Blandamer, M. J. *J. Phys. Org. Chem.* **1998**, *11*, 841−846.
(46) Stanley, C. B.; Rau, D. C. *Biophys. J.* **2006**, *91*, 912−920.
(47) Flock, S.; Labarbe, R.; Houssier, C. *Biophys. J.* **1996**, *70*, 1456−1465.
(48) Mel'niov, S. M.; Khan, M. O.; Lindman, B.; Jönsson, B. *J. Am. Chem. Soc.* **1999**, *121*, 1130−1136.
(49) Naimushin, A. N.; Quach, N.; Fujimoto, B. S.; Schurr, J. M. *Biopolymers* **2001**, *58*, 204−217.
(50) de Souza, F. P.; Neto, A. A.; Fossey, M. A.; Neto, J. R. *Biopolymers* **2007**, *87*, 244−248.
(51) Vergara, A.; Annunziata, O.; Paduano, L.; Miller, D. G.; Albright, J. G.; Sartorio, R. *J. Phys. Chem. B* **2004**, *108*, 2764−2772.
(52) Asami, K.; Hanai, T.; Koizumi, N. *J. Membr. Biol.* **1976**, *28*, 169−180.
(53) Tanizaki, S.; Clifford, J.; Connelly, B. D.; Feig, M. *Biophys. J.* **2008**, *94*, 747−759.